CHAPTER 3

CONTACT ANGLES OF POWDERS FROM HEAT OF IMMERSION

3.1 INTRODUCTION

Many industrial processes depend on controlling the hydrophobicity of the solids involved. These include flotation (1-3), wetting (4), filtration (5), adhesion (6) etc. The most commonly used measure of hydrophobicity is water contact angle (θ) (7-9). It can be readily measured by placing a drop of water on the surface of a solid of interest, and measure the angle through the aqueous phase at the three-phase contact. In using this method, known as sessile drop technique, it is necessary that the solid surface be flat and smooth. To meet these requirements, a mineral specimen is cut by a diamond saw and polished with an abrasive powder such as alumina. It is well known, however, that mineral surfaces particularly those of sulfide minerals undergo significant chemical changes and atomic rearrangements during polishing. Therefore, it would be more desirable to measure contact angles directly on powdered samples. Some times, the solids of interest exist only in powdered form, in which case the sessile drop technique cannot be used for contact angle measurements. It is also unreliable and impractical to use the conventional contact angle measurement techniques for the characterization of fine powders such as fillers, pigments and fibers.

For powdered samples, capillary rise technique is widely used (10-12). In this technique, a powdered solid is packed into a capillary tubing, one end of which is subsequently immersed into a liquid of known surface tension. The liquid will rise through the capillaries formed in between the particles within the tubing. The distance, l, traveled by the liquid as a function of time t is measured. If one knows the mean radius r^* of the capillaries present in the tubing, he can calculate the contact angle using the Washburn equation (13, 14):

$$l^2 = \frac{\gamma_{LV} r^* t \cos\theta}{2\eta} \qquad [3.1]$$

where η is the liquid viscosity. One can determine r^* with a liquid which completely wets the powder, i.e., $\theta=0$. One problem with this technique is the uncertainty associated with determining r^*. There is no guarantee that the value of r^* determined with a completely wetting liquid is the same as that determined by a less than completely wetting liquid. Also, the method of using the Washburn equation gives only advancing contact angles rather than equilibrium angles.

The Washburn equation is also used in thin layer wicking method (15-16). In this technique, a powdered sample is deposited on a glass slide and dried. One end of the slide coated with the dry powder is immersed in wetting liquid, and the rate at which the liquid rises along the height of the slide is measured.

The contact angle of a powdered sample can also be measured by compressing it into a pellet. The measured values may vary depending on the roughness and porosity of the pellet. There is also a concern that the particles in the top layer of a pellet may be deformed during compression, which may also affect the measurement (17).

Another method of determining the contact angles of powders is to measure the heat of immersional wetting in various testing liquids, e.g. water, formamide etc. In this technique, a powdered sample is degassed to remove the pre-adsorbed water and then immersed in liquid (11, 18-22). In general, the more hydrophobic a solid is, the lower the heat of immersion in water. Thus, one should be able to obtain the values of contact angles from the heats of immersion in water. Different investigators use different methods of calculating contact angles from the heat of immersion (20-22). Some of the methods reported in the literature used gross assumptions, which may be the source of inaccuracy in determining water contact angles.

It was the purpose of this chapter to develop a method of determining the contact angles of powdered talc samples from the values of calorimetric heats of immersion measurements. It is based on using a more rigorous thermodynamic relation. The contact angles were then used to determine the surface free energies of the talc samples using the Van Oss-Chaudhury-Good equation.

3.2 THEORY

3.2.1 Contact Angles from Heat of Immersion

In the present work, a Microscal flow microcalorimeter was used to measure the heat effect (h_i) created when a powdered sample was immersed in liquid. By dividing h_i with the total surface area of the sample used in the experiment, one obtains the heat of immersional wetting enthalpy ($-\Delta H_i$) given in units of mJ/m^2.

In the wetting experiment, a powdered sample was evacuated before the immersion. Therefore, the free energy (ΔG_i) of immersion is given by the following relationship:

$$\Delta G_i = \gamma_{SL} - \gamma_S \qquad [3.2]$$

where γ_{SL} is the solid-liquid interfacial tension and γ_S is the surface free energy of the solid, which is in equilibrium with its own vapor.

The enthalpy of immersion (ΔH_i) determined using the heat of immersion measurements can be related to ΔG_i as follows:

$$\Delta H_i = \Delta G_i - T\left(\frac{d\Delta G_i}{dT}\right)_p \qquad [3.3]$$

where T is the absolute temperature. Substituting Eq. [3.2] into Eq. [3.3], one obtains:

$$\Delta H_i = (\gamma_{SL} - \gamma_S) - T\left[\frac{d(\gamma_{SL} - \gamma_S)}{dT}\right]_p \qquad [3.4]$$

One can substitute γ_{SL}-γ_S with $-\gamma_L\cos\theta$ from Young's equation to obtain:

$$\Delta H_i = -\gamma_{LV}\cos\theta + T\left[\frac{\partial(\gamma_{LV}\cos\theta)}{\partial T}\right]_p$$
$$= -\gamma_{LV}\cos\theta + T\left[\cos\theta\left(\frac{\partial\gamma_{LV}}{\partial T}\right)_p + \gamma_{LV}\left(\frac{\partial\cos\theta}{\partial T}\right)_p\right] \quad [3.5]$$
$$= -\cos\theta\left[\gamma_{LV} - T\left(\frac{\partial\gamma_{LV}}{\partial T}\right)_p\right] + \gamma_{LV}T\left(\frac{\partial\cos\theta}{\partial T}\right)_p$$

where θ is the contact angle.

Since the enthalpy of the liquid (H_L) is given by

$$H_L = \gamma_{LV} - T\left(\frac{\partial\gamma_{LV}}{\partial T}\right)_p, \quad [3.6]$$

Eq. [3.5] is reduced to:

$$\Delta H_i = -H_L\cos\theta + \gamma_{LV}T\left(\frac{\partial\cos\theta}{\partial T}\right)_p \quad [3.7]$$

Solving Eq. [3.7] for $\cos\theta$, one obtains the following relationship:

$$\cos\theta = \frac{1}{H_L}\left[\gamma_{LV}T\left(\frac{\partial\cos\theta}{\partial T}\right)_p - \Delta H_i\right] \quad [3.8]$$

which is a first-order differential equation with respect to $\cos\theta$.

There are no analytical solutions for Eq. [3.8]. Numerical solutions are possible, provided that a value of contact angle is known at one particular temperature. Nevertheless, Eq. [3.8] can be useful for determining θ from the value of ΔH_i determined using a calorimeter. For this to be possible, it is necessary to have the values of H_L, γ_{LV} and $\partial cos\theta/\partial T$

for a given liquid at a given temperature. The first two are usually available in the literature, and the temperature coefficient of contact angles can be determined from experiment.

There are several ways of determining temperature coefficient of $cos\theta$. *First*, one measures θ on polished talc samples as a function of temperature and determine $\partial cos\theta/\partial T$ experimentally. An assumption made here is that although contact angle may change when it is pulverized, its temperature coefficient may remain the same. *Second*, the contact angle of a powdered sample is measured by pressing it into a pellet. Again, the pressed talc sample may have a different contact angle from that of loose powders. However, its temperature coefficient may be assumed to remain the same. *Third*, the contact angles of powdered samples are measured using the capillary rise technique. This technique gives advancing rather than equilibrium contact angles. If one uses this technique to determine $\partial cos\theta/\partial T$, an implicit assumption is that the temperature coefficients of the equilibrium and the advancing angles are the same.

3.2.2 Van Oss-Chaudhury-Good (VCG) Equation

The contact angles obtained from microcalorimetric measurements can be used for characterizing the talc surface in terms of its surface free energy components. Essentially, the method of characterizing the talc surface is based on using the Van Oss-Good-Chaudhury equation (23-25):

$$(1+\cos\theta)\gamma_L = 2\left(\sqrt{\gamma_S^{LW}\gamma_L^{LW}} + \sqrt{\gamma_S^{+}\gamma_L^{-}} + \sqrt{\gamma_S^{-}\gamma_L^{+}}\right), \qquad [3.9]$$

which is useful for determining the surface free energy (γ_S) and its components (i.e., γ_S^{LW}, γ_S^{+}, and γ_S^{-}) on a solid surface. To obtain these values, it is necessary to determine contact angles of three different liquids of known properties (in terms of γ_L^{+}, γ_L^{-}, γ_L^{LW}) on the surface of the solid of interest. One can then set up three equations with three unknowns, which can be solved to obtain the values of γ_S^{LW}, γ_S^{+}, and γ_S^{-}. Once the values of γ_S^{LW}, γ_S^{+}, and γ_S^{-} are known, one can determine the values of γ_S^{AB} and γ_S using the following equations:

$$\gamma_S = \gamma_S^{LW} + \gamma_S^{AB}$$

$$= \gamma_S^{LW} + 2\sqrt{\gamma_S^+ \gamma_S^-} \qquad [3.10]$$

Thus, the values of $\gamma_S, \gamma_S^{LW}, \gamma_S^{AB}, \gamma_S^+,$ and γ_S^- for each talc surface can be determined using Eqs. [3.9] and [3.10].

3.3 EXPERIMENTAL

3.3.1 Materials

A run-of-the-mine (ROM) talc sample from Montana was received from Luzenac America. It was crushed to -50 mm using a hand-held hammer. One part was kept for contact angle measurements using the sessile drop and the Wilhelmy plate techniques on flat surfaces, while the other part was ground to -150 μm using an agate mortar and pestle. The ground samples were used for i) heat of immersion measurement using a flow microcalorimeter and ii) contact angle measurements using the capillary rise technique.

A number of powdered talc samples were also obtained from Luzenac America. These commercial products were named: i) Yellowstone, ii) Mistron-100, iii) Mistron Vapor-P, and iv) Select-A-Sorb. These samples were used in the present work as received.

In the present work, four different solvents were used for the heat of immersion measurements. These include: toluen, n-heptane, formamide and water. All of them were HPLC grade. Toluen and n-heptane were obtained from Aldrich Chemical Company and, formamide was purchased from Fisher Scientific. They were dried overnight over 3 to 12 mesh Davidson 3-A molecular sieves before use. All heats of immersion measurements were conducted using Nanopure water produced from a Barnsted Nanopure II water purification system. All the glassware was oven-dried for at least 24 hours at 75 ^{o}C prior to use. The syringe, calorimeter cell, fittings and the teflon tubing lines of the microcalorimeter were cleaned using HPLC grade acetone (Fisher Scientific) after each run. Heat of immersion experiments were conducted at 20±2 ^{o}C.

3.3.2 Experimental Apparatus and Procedure

Heats of immersion measurements were conducted using a flow microcalorimeter (FMC) from Microscal, United Kingdom, as shown in Figure 3.1. A schematic diagram of the microcalorimeter is illustrated in Figure 3.2. A calorimeter cell, made of Teflon, was placed in a metal block, which was insulated from the ambient by mineral wool. Two glass-encapsulated thermistors were placed inside the cell to monitor the changes in temperature of the sample, and two reference thermistors were placed in the metal block outside the cell. The calorimeter was calibrated by means of a calibration coil, which was placed in the sample bed. The entire unit was housed in a draft-proof enclosure to reduce the effect of temperature fluctuations in the ambient.

In each measurement, a talc sample was dried overnight in an oven at 110 ^{o}C. A known amount (usually 0.05-0.15 gram) of the dried sample was placed in the calorimeter cell, and degassed for at least 30 minutes under vacuum (<5 mbar) at ambient temperature. The vacuum system consisted of a vacuum pump and a liquid nitrogen vapor trap. The solvent was then introduced to the calorimeter cell at a steady flow rate of 3.3 ml/h by means of a syringe micropump, and the heat effect was recorded by means of a strip chart recorder and a PC. Thermal equilibrium was reached usually 8 to 30 minutes, depending on the powder and liquid used. The recorded experimental data was analyzed using the Microscal Calorimeter Digital Output-Processing System (CALDOS). This program enables the analysis of the calibration and experimental data and converts the raw downloaded data into the heat of immersion (h_i).

3.4 RESULTS AND DISCUSSION

3.4.1 Surface Area and Particle Size

Table 3.1 gives the values of the BET specific surface area and average particle size (d_{50}) for the samples used in the present work. The surface area measurements were conducted using a Nova-1000 Surface Area Analyzer (Quantachrome Corporation) with nitrogen as adsorbate. The value of d_{50} was determined by sieve analysis for the Montana talc, while those of the rest of the samples were provided from Luzenac America. Figure 3.3

shows a plot of surface area vs. $1/d_{50}$. As shown, most of the points are in line suggesting that as the particle size goes down the surface area increases in a linear fashion.

3.4.2 Heats of Immersion

Figure 3.4 shows a typical thermogram obtained from the flow microcalorimeter. Also shown is a thermogram created calibration purposes. This particular experiment is for the heat of immersion of a run-of-mine Montana talc sample in water.

Table 3.2 shows the results of the heats of immersion measurements conducted on the various talc samples using water, formamide, toluene and n-heptane as the test liquids. The surface tensions and their components for the liquids (γ_L^{LW}, γ_L^{AB}, γ_L^+, γ_L^-) are given in Chapter 2 (Table 2.1).

As shown in Table 3.2, the values of heat of immersion enthalpies in water were in the range from 220-322 mJ/m^2. It is interesting that the enthalpy of immersion in water was related to the particle size of the sample. As shown, it was most negative with the run-of-mine Montana talc sample (d_{50}=63 μm), and the least negative with Select-A-Sorb (d_{50}=3.5 μm). This observation may be related to the fact that the finer the particles, the larger the aspect ratio. The particles with higher aspect ratios should give lower heats of immersion, as larger proportions of the surface area are due to the basal plane that is hydrophobic.

The value of heat of immersion enthalpy in water obtained for the run-of-mine Montana talc is comparable to those reported by Malandrini et al (20) for a variety of run-of-mine European talc samples. However, the values obtained with very fine talc powders (e.g. Select-A-Sorb, Mistron Vapor-P) were substantially lower than reported by the same authors (20). The lower values of heat of immersion enthalpies in water obtained with fine samples should be attributed to the increased hydrophobicity of talc surface upon grinding.

As shown in Table 3.2, a similar relationship can also be established between the particle size and the heat of immersion enthalpies for formamide. As shown, the enthalpy of immersion was most negative with the run-of-mine Montana talc sample (156.7 mJ/m^2), and the least negative with Select-A-Sorb (42.9 mJ/m^2). Since formamide is known to be the most basic polar liquid, the results indicate that the surface acidity of the particles increases with increasing particle size. It should be pointed out that the heats of immersion obtained here are substantially lower than those reported by Malandrini et al (20) for formamide. The

discrepancy may be attributed to the differences in origin, particle size, sample preparation technique etc.

It can also be seen from Table 3.2 that the values of heat of immersion enthalpies for n-heptane were in the range from 66.4-88.2 mJ/m^2. Note that n-heptane interacts only with the basal surface of talc and the interaction between talc surface and n-heptane is only through the Lifshitz-van der Waals interaction. Therefore, the heat of immersion given in terms of mJ/m^2 should be more or less the same. The data suggest that the basal surface of Mistron Vapor-P is most hydrophobic.

3.4.3 Contact Angles From Heat of Immersion

Eq. [3.8] was used to calculate the contact angles of water and formamide on the powdered talc samples. In using this equation, the values of ΔH_i given in Table 3.2 were used, while the values of H_L for water (119.16 mJ/m^2) and formamide (107.8 mJ/m^2) were taken form the literature (26). The surface tension values were taken from Table 2.1. The values of $\partial\cos\theta/\partial T$ both for water and formamide were determined by conducting contact angle measurements as a function of temperature.

Figure 3.4 shows the results of the contact angle measurements for water conducted on the flat Montana talc specimen using the Wilhelmy plate technique in the temperature range of 15-25^oC. Figure 3.5 shows the results of the same measurements obtained for formamide. Wilhelmy plate technique gives both advancing and receding angles. For the powdered samples, the contact angle measurements were conducted using the capillary rise technique, and the results are given in Figure 3.6 for water and in Figure 3.7 for formamide, respectively. It is commonly believed that the capillary rise technique gives advancing contact angles (17). As shown, contact angles decreased with increasing temperature. From the slope, the values of $\partial\cos\theta/\partial T$ were obtained and are given in Table 3.3 for water and Table 3.4 for formamide, respectively.

As it can be seen in Table 3.3, for the Montana talc sample, the Wilhelmy plate technique gave a substantially higher value of $\partial\cos\theta/\partial T$ than the capillary rise technique. This discrepancy may be explained as follows. It is likely that the flat Montana talc sample may have more hydrophilic sites exposed on the surface. As has already been discussed in Chapter 2, the finer a talc sample is, the more hydrophobic it becomes. This was attributed to

the likelihood that talc particles break preferentially along the basal plane, thereby exposing a larger proportion of the hydrophobic basal planes. Thus, the smaller the particle size, the more hydrophobic the particles would become, and less strongly the water molecules would adsorb on the surface. As the temperature increases, the bonding between the water and the hydrophilic surface should become weaker. Therefore, $\partial\theta/\partial T$ should be negative, as shown in the present work. They should become more negative when a talc surface becomes more hydrophilic. Indeed, the results given in Figure 3.6 shows that $\partial\theta/\partial T$ becomes increasingly negative with decreasing θ.

It is interesting to note that the values of $\partial\cos\theta/\partial T$ obtained for formamide are in the same order of magnitude with those obtained for water. As shown in Table 3.4, the values of $\partial\cos\theta/\partial T$ determined using capillary rise technique were substantially higher than those obtained using the Wilhelmy plate technique, which is similar to those obtained with water. The results given in Table 3.4 also suggest that the adsorption strength of the formamide molecules decreases with decreasing particle size. Therefore, as shown in Figure 3.7, the slope of $\partial\theta/\partial T$ becomes less negative with decreasing particle size.

For the reasons given above, it was decided to use the values of $\partial\cos\theta/\partial T$ obtained using the capillary rise technique rather than those from Wilhelmy plate technique for calculating water and formamide contact angles (θ) from the values of $-\Delta H_i$ using Equation [3.8]. The calculated contact angle values for water are given in Table 3.5, while those obtained for formamide are given in Table 3.6. Also shown in the tables for comparison are the values of θ obtained using the capillary rise and Wilhelmy plate methods.

It can be seen from Table 3.5 that the values of water contact angles determined from the heat of immersion data are in the range of 66 to 78^o. These are substantially larger than the values of 29-59^o reported by Malandrini et al (20) for several different European talc samples at 20 ^{o}C. These authors also used the heats of immersion methods. The low contact angles of the European talc samples agrees with the fact that their heats of immersion values were larger than those of the North American talc samples measured in the present work. For example, the European talc samples gave the values of heats of immersion to be in the range of 311 to 356 mJ/m^2, whereas the North American talc samples gave the values as low as 220 mJ/m^2 (for Select-A-Sorb powder). These results indicate that North American talc samples are more hydrophobic than the European talc. The level of impurities (e.g. chlorite)

found in European talc samples is higher than the North American talc. That should have an effect on the surface hydrophobicity of talc.

The contact angles obtained from the heat of immersion measurements may be considered to be equilibrium angles, as was suggested by Spagnolo, et al (21) and Yan, et al (22). In this regard, they should be smaller than those obtained using the capillary rise technique. This is actually the case with the Montana talc and Select-A-Sorb samples. However, the values of contact angles obtained for the Yellowstone, Mistron-100, and Mistron Vapor-P using the heat of immersion technique are close to those obtained using the capillary rise technique, which gives advancing angles. The only possible explanation may be that the surfaces of these samples were smoother and more homogenous than the others, in which case the difference between advancing and equilibrium angles can be small.

The contact angles given in Table 3.6 for formamide show somewhat different trend. The advancing contact angle value obtained using capillary rise technique with Montana talc and Mistron-100 powders are higher than those of equilibrium contact angles obtained from microcalorimetric measurements. The values of contact angles for the other powders are close to each other, suggesting the smoothness and homogeneity of these surfaces.

One of the most important advantages of using the heat of immersion technique over the capillary rise technique is probably that it gives more reproducible results. As shown in Tables 3.5 and 3.6, the former gave considerably smaller margins of error. It seems that it is as reproducible as the Wilhelmy plate technique. However, the latter cannot be used for powdered samples.

The data given in Figure 3.7 shows an interesting trend. As talc samples become more hydrophobic the θ vs. T plots becomes increasingly flat. With Select-A-Sorb, whose $\theta \approx 90^o$, the $\partial\theta/\partial T$ (and, hence, $\partial\cos\theta/\partial T$) zero. It follows then that Eq. [3.8] is reduced to

$$\cos\theta = -\frac{\Delta H_i}{H_L}, \qquad [3.11]$$

which in turn suggests that heat of immersion ($-\Delta H_i$) should become zero at $\theta=90^o$. Eq. [3.9] suggests also that at $\theta>90^o$, the heat effect should become endothermic. Spagnolo et al (21) indeed showed experimentally that the heats of immersion of two fluorinated hydrocarbon

powders in water became endothermic. The two fluorinated hydrocarbons had water contact angles of 120 and 125°. This finding suggest that water molecules are not bonded strongly at $\theta > 90^{o}$.

3.4.4 Surface Free Energy Components of Talc from Microcalorimetric Measurements

The values of contact angles obtained from microcalorimetric measurements, as given in Table 3.5 for water and Table 3.6 for formamide, were used for determining the surface free energies (γ_S) of the talc samples and their components (γ_S^{LW}, γ_S^{AB}, γ_S^{+}, γ_S^{-}) using Van Oss-Chaudhury-Good equation (Eq. [3.9]). To do this, it was necessary to determine the contact angles of three different liquids of known properties (in terms of γ_L^{+}, γ_L^{-}, γ_L^{LW}) on the surface of the solid of interest. Thus, the values of γ_S^{LW}, γ_S^{+}, and γ_S^{-} could be calculated by solving three equations simultaneously.

Table 3.5 and 3.6 give the contact angle values for water and formamide, respectively. For the calculation, n-heptane was chosen to be the third liquid. However, the contact angle measurements conducted with n-heptane showed that it completely spreads over the talc surface, thus yielding a zero contact angle value. Since n-heptane completely spreads over talc, it was not possible to determine θ from ΔH_i as we don't have the value of $\partial\cos\theta/\partial T$. For this reason, the value of γ_S^{LW} on the talc surface was determined from the value of heat of immersion enthalpies for n-heptane using the equation derived as follows:

Van Oss et al (23, 27-28) showed that the interfacial tension (γ_{SL}) at a solid-liquid interface can be given by the following relationship:

$$\gamma_{SL} = \gamma_S + \gamma_L - 2\left(\sqrt{\gamma_S^{LW}\gamma_L^{LW}} + \sqrt{\gamma_S^{+}\gamma_L^{-}} + \sqrt{\gamma_S^{-}\gamma_L^{+}}\right) \qquad [3.12]$$

Substituting Eq. [3.12] into Eq. [3.2], one obtains:

$$\Delta G_i = \gamma_L - 2\left(\sqrt{\gamma_S^{LW}\gamma_L^{LW}} + \sqrt{\gamma_S^{+}\gamma_L^{-}} + \sqrt{\gamma_S^{-}\gamma_L^{+}}\right) \qquad [3.13]$$

For an apolar liquid interacting with a solid, Eq. [3.13] becomes:

$$\Delta G_i = \gamma_L - 2\sqrt{\gamma_S^{LW}\gamma_L^{LW}} \qquad [3.14]$$

Eq. [3.14] suggests that as the value of γ_S^{LW} becomes smaller, the Gibbs free energy of immersion becomes also smaller, indicating the surface hydrophobicity of the solid.

Substituting Eq. [3.14] into Eq. [3.3] and differentiating it with respect to temperature, one obtains,

$$\Delta H_i = \gamma_L - 2\sqrt{\gamma_L^{LW}\gamma_S^{LW}} - T\frac{\partial\gamma_L}{\partial T} + 2T\sqrt{\gamma_L^{LW}}\frac{\partial\sqrt{\gamma_S^{LW}}}{\partial T} + 2T\sqrt{\gamma_S^{LW}}\frac{\partial\sqrt{\gamma_L^{LW}}}{\partial T} \qquad [3.15]$$

which was originally derived by Fowkes (19). This equation allows one to determine γ_S^{LW} from the values of heat of immersion ($-\Delta H_i$), γ_L, γ_L^{LW}, and the temperature coefficients of the liquid and solid involved. The temperature coefficients of γ_L and γ_L^{LW} are usually available from the literature, while that of γ_S^{LW} may be assumed to be zero (19). In using Eq. [3.15], the values of $\partial\gamma_L/\partial T = 0.098$ and $\partial\gamma_L^{LW}/\partial T = 0.098$ for n-heptane were taken from the literature (26). The heats of immersion values ($-\Delta H_i$) for n-heptane were taken from Table 3.2.

Table 3.7 shows the values of γ_S^+ and γ_S^- obtained by solving Eq. [3.9], along with the values of γ_S^{LW} determined using Eq. [3.15]. The values of γ_S^{AB} and γ_S given in the last two columns of the table were obtained using Eq. [3.10].

As shown, the value of γ_S^- is much higher than the value of γ_S^+ for all five talc samples studied. The results given in this table also suggest that the value of γ_S^- may change from one talc to another, while the value of γ_S^+ remains practically constant. Likewise, the surface free energy components obtained from the direct contact angle measurements using various techniques showed that a talc surface free energy contains both acid and basic component, the basic component being in the majority (see Chapter 2). Thus, the results obtained from the microcalorimetric measurements are in good agreement with those obtained using other methods.

Also shown, the surface free energy of all of the five talc samples studied consists predominantly of Lifshitz-van der Waals surface free energy component (γ_S^{LW}). The values

of γ_S^{AB} are small. This explains why the surface of talc is nonpolar or hydrophobic. The results given in Table 3.7 also suggest that the surface free energy (γ_S) of talc decreases with decreasing particle size, which is consistent with those observed using other methods, as reported in Chapter 2.

Furthermore, the results presented in this chapter and also in the previous chapters suggest that the value of heat of immersion enthalpy in water is strictly dependent on the surface hydrophobicity (θ_a). From this standpoint, a relationship was established between advancing water contact angles measured using various direct measurement techniques (e.g. capillary rise, thin layer wicking) and, the heat of immersion enthalpies and the surface free energy parameters of various talc powders. The results are summarized in Figure 3.9, where the values of heat of immersion enthalpies were taken from Table 3.2, the values of θ_a were obtained from Tables 2.6 and 2.7 and the values of γ_S, γ_S^{LW}, γ_S^-, γ_S^+ and γ_S^{AB} were taken from Tables 2.10 and 2.12.

Figure 3.9 shows that the value of heat of immersion enthalpy decreases as θ_a increases. It has to be pointed out that the increase in the value of θ_a is primarily achieved due to a decrease in the value of γ_S^{LW} and, hence, a decrease in the value of γ_S. For example, γ_S^{LW} was 31.0 mJ/m^2 at θ_a =82^o and further decreased to a value of 17.8 mJ/m^2 at θ_a =89.4^o. On the other hand, γ_S^{AB} remained practically constant at the whole contact angle range.

According to Figure 3.9, the value of γ_S^- increases, while the value of γ_S^+ slightly decreases with increasing θ_a. Since the γ_S^{AB} is given by $\gamma_S^{AB} = 2\sqrt{\gamma_S^+ \gamma_S^-}$ (Eq. [3.10]), it should be expected that the value of γ_S^{AB} should remain unchanged as one of the components in Eq. [3.10] increases, while the other decreases. It may be questioned what really causes an increase in the value of γ_S^- and a decrease in the value of γ_S^+ with increased θ_a. It has already been shown that the area of hydrophobic basal plane surfaces increases and the area of hydrophilic edge surfaces decreases as the surface becomes more hydrophobic, i.e, θ_a increases. Therefore, one plausible explanation for the increase in the value of γ_S^- with increased θ_a would be that the surfaces of basal planes contains predominantly the basic component (γ_S^-), while the edge surfaces contains mainly the acidic component (γ_S^+). This point will be made clear in the next chapter.

3.5 CONCLUSIONS

An improved method of determining the contact angles of water and formamide on powdered samples has been presented in the present work. It is based on measuring the heats of immersion, and calculating contact angles using a rigorous thermodynamic relation. The method of calculating contact angles was tested on a series of talc samples from Luzenac America. The results obtained using the calorimetric method are comparable to those obtained using the capillary rise technique. However, the calorimetric technique produced more reproducible results.

The contact angle data obtained from the microcalorimetric measurements have been used to determine the surface free energies (γ_S) and their components (γ_S^{LW}, γ_S^-, γ_S^+) for five different talc samples from Luzenac America. The results show that the van der Waals component (γ_S^{LW}) comprises the largest part of the surface free energy with small acid-base components, which explains the hydrophobic properties of talc. The surface free energy data also show that all of the talc samples are basic, which suggests that they can serve as excellent adsorbents for acidic adsorbates.

The data obtained in the present work show that the smaller the particle size, the more hydrophobic a talc sample becomes. This observation may be attributed to the likelihood that the small particles have higher aspect ratios, which in turn may be ascribed to the preferential breakage of talc particles along the basal plane.

The results showed that the surface of talc contains both basic and acidic sites. However, the number of basic sites is much larger than the number of acidic sites as defined from the contact angle measurements and by the application of VCG equation.

As a general trend, the γ_S^{LW} component of surface free energy decreases with decreasing particle size, and so does the value of γ_S. However, the γ_S^{LW} component remains practically constant. A linkage between particle hydrophobicity and surface free energy components was established. The more the hydrophobic surface is the lower the γ_S is.

3.6 REFERENCES

1. Aplan, F. F., and Fuerstenau, D. W., *Froth Flotation*, 50th Anniversary Volume, Ed.: D. W. Fuersteanu, AIME, New York, 1962.

2. Leja, J., *Surface Chemistry of Froth Flotation*, Plenum Press, New York, 1982.
3. Yoon, R.-H., Aufbereitungs-Technik, 32, 474, 1991.
4. Adamson, A. W. and Gast, A.P., *Physical Chemistry of Surfaces,* 6th ed., John Wiley and Sons, 1997.
5. Basim, B., and Yoon, R.-H., *SME Annual Meeting*, Salt Lake City, UT, 2000.
6. Zisman, W. A., in: *Handbook of Adhesives*, Skeist, I., Ed: van Nostrand, NewYork, Chapter 3, 1977.
7. Fuerstenau, D. W., *Mining Engineering*, Transactions AIME, December, pp. 1367-1367, 1957.
8. Yoon, R.-H., and Ravishankar, S. A., *J. Colloid Interface Science*, 179, 391, 1996.
9. Yoon, R.-H., and Pazhianur, R., *Colloid Surfaces*, 1999.
10. Bruil, H. G., and van Aartsen, J. J., *Colloid and Polymer Science*, 252, 32-38, 1974.
11. Hansford, D. T., Grant, D. J. W., and Newton, J. M., *J. C. S. Faraday Trans. I*, 76, 2417-2431, 1980.
12. Crawford, R., Koopal, L. K., and Ralston, J., *Colloids and Surfaces*, 27, 57-64, 1987.
13. Washburn, E. W., *Physical Review*, 1, pp. 273, 1921.
14. Davies, J. T., Rideal, E. K., *Interfacial Phenomena*, (New York), 423 (1963).
15. van Oss, J. C., Giese, R. F., Li, Z., Murphy, K., Norris, J., Chaudhury, M. K., and Good, R. J., *J. Adhesion Sci. Technol.*, Vol. 6, No. 4, pp. 413-428, 1992.
16. Wu, W., Griese, R.F. Jr., and van Oss C.J., *Powder Technology*, 89, 129-132, 1996.
17. Neumann, A. W., and Good, R. J., in: *Surface and Colloid Science*, Eds: R.J. Good and R.R. Stromberg, vol. 11, p.31. Plenum, New York, 1979.
18. Young, G. J., Chessick, J. J., Healey, F. H., and Zettlemoyer, A. C., *J. Phys. Chem.*, 58, 313, 1954.
19. Fowkes, F.M., *Ind. and Eng. Chem.*, 56/12, 40, 1964.
20. Malandrini, H., Clauss, F., Partyka, S., and Douillard, J. M., *J. Colloid and Interface Sci.,* 194, 183-193, 1997.
21. Spagnolo, D. A., Maham, Y., Chuang, K. T., *J of Physical Chemistry*, 100, 6626, 1995.
22. Yan, N., Maham, Y., Masliyah, J. H., Gray, M., and Mather , A. E., *J of Colloid and Interface Sci.*, 228, pp.1-6, 2000.

23. Van Oss, C. J., Good, R. J., and Chaudhury, M. K., *J. of Colloid and Interface Science*, 111, pp. 378, 1986.
24. Van Oss, C. J., Chaudhury, M. K., and Good, R. J., *J. of Colloid and Interface Science*, 128, 313, 1988.
25. Van Oss, C. J., Giese, R.F., Good, R. J., *Langmuir*, 6, pp. 1711-1713, 1990.
26. Weast, R. C., Astle, M. J., (Eds.), *Handbook of Phys. Chem.*, 61st ed., CRS Press, Inc., Boca Baton, FL, 1981.
27. Van Oss, C. J., Chaudhury, M. K., and Busscher, H., *J. of Dispersion Sci. Technol.*, 11, 77, 1990.
28. Van Oss, C. J., *Interfacial Forces in Aqueous Media*, Marcel Decker Inc., New York, 1994.

Table 3.1. Specific surface areas and average particle size of the studied talc samples

Talc Sample	Surface Area (m^2/g)	d_{50} (μm)
Montana ROM	7.65	63
Yellowstone	9.5	12.5
Mistron-100	13.0	3.5
Mistron Vapor-P	13.0	3.0
Select-A-Sorb	11.0	3.4

Table 3.2. The heat of immersion enthalpies of various liquids on talc samples studied (20±2 °C)

Talc Sample	$-\Delta H_i$ (mJ/m^2)			
	Water	Formamide	Toluen	n-Heptane
Montana-ROM(*)	322	156.7	278.5	88.2
Yellowstone	297	57.6	251.5	76.1
Mistron-100	293	81.8	217.4	82.7
Mistron Vapor-P	237	45.4	178.7	66.4
Select-A-Sorb	220	42.9	157.2	68.2

(*) 75 x 53 μm fraction was used in the experiments

Table 3.3. The value of $\partial\cos\theta/\partial T$ for water on various talc surfaces obtained using Wilhelmy plate and capillary rise techniques

Talc Sample	$\partial\cos\theta/\partial T$ for Water	
	Wilhelmy Plate	Capillary Rise
Montana	4.55×10^{-3}	3.0×10^{-4}
Yellowstone	--	6.8×10^{-4}
Mistron-100	--	3.4×10^{-4}
Mistron Vapor-P	--	3.8×10^{-4}
Select-A-Sorb	--	2.1×10^{-4}

Table 3.4. The value of $\partial\cos\theta/\partial T$ for formamide on various talc surfaces obtained using Wilhelmy plate and capillary rise techniques

Talc Sample	$\partial\cos\theta/\partial T$ for Water	
	Wilhelmy Plate	Capillary Rise
Montana	3.1×10^{-3}	5.5×10^{-4}
Yellowstone	--	7.8×10^{-4}
Mistron-100	--	4.9×10^{-4}
Mistron Vapor-P	--	5.9×10^{-4}
Select-A-Sorb	--	9.5×10^{-4}

Table 3.5. Comparison of the water contact angles calculated using Eq. [3.8] with those obtained using other methods (at 20±2 ^{o}C)

Talc Sample	From Eq. [3.8] ($\theta_{eq.}$)	Capillary Rise ($\theta_{adv.}$)	Wihelmy Plate ($\theta_{adv.}$)
Montana-ROM	66.0±2.1	82.3±4.5	69.7±2
Yellowstone	67.4±1.8	69.7±5.3	--
Mistron-100	75.5±1.5	74.0±3.8	--
Mistron Vapor-P	77.2±1.6	77.9±4.7	--
Select-A-Sorb	78.1±2.0	89.9±2.4	--

Table 3.6. Comparison of the formamide contact angles calculated using Eq. [3.8] with those obtained using other methods (at 20±2 ^{o}C)

Talc Sample	From Eq. [3.8] ($\theta_{eq.}$)	Capillary Rise ($\theta_{adv.}$)	Wihelmy Plate ($\theta_{adv.}$)
Montana-ROM	46.9±2.2	56.1±3.5	49.8±1.8
Yellowstone	46.1±1.8	43.7±5.0	--
Mistron-100	37.4±2.0	47.9±4.8	--
Mistron Vapor-P	59.2±1.7	58.7±4.5	--
Select-A-Sorb	64.2±1.9	61.4±4.2	--

Table 3.7. Surface free energy components of talc samples obtained from microcalorimetric measurements

Talc Sample	Surface Free Energy, mJ/m^2				
	γ_S^{LW}	γ_S^+	γ_S^-	γ_S^{AB}	γ_S
Montana-ROM	53.4	0.2	14.5	3.3	56.7
Mistron-100	46.3	1.2	2.7	3.6	49.9
Yellowstone	38.4	0.7	11.4	5.7	44.1
Mistron Vapor-P	28.2	1.04	7.8	5.7	33.9
Select-A-Sorb	30.0	0.34	9.3	3.2	33.2

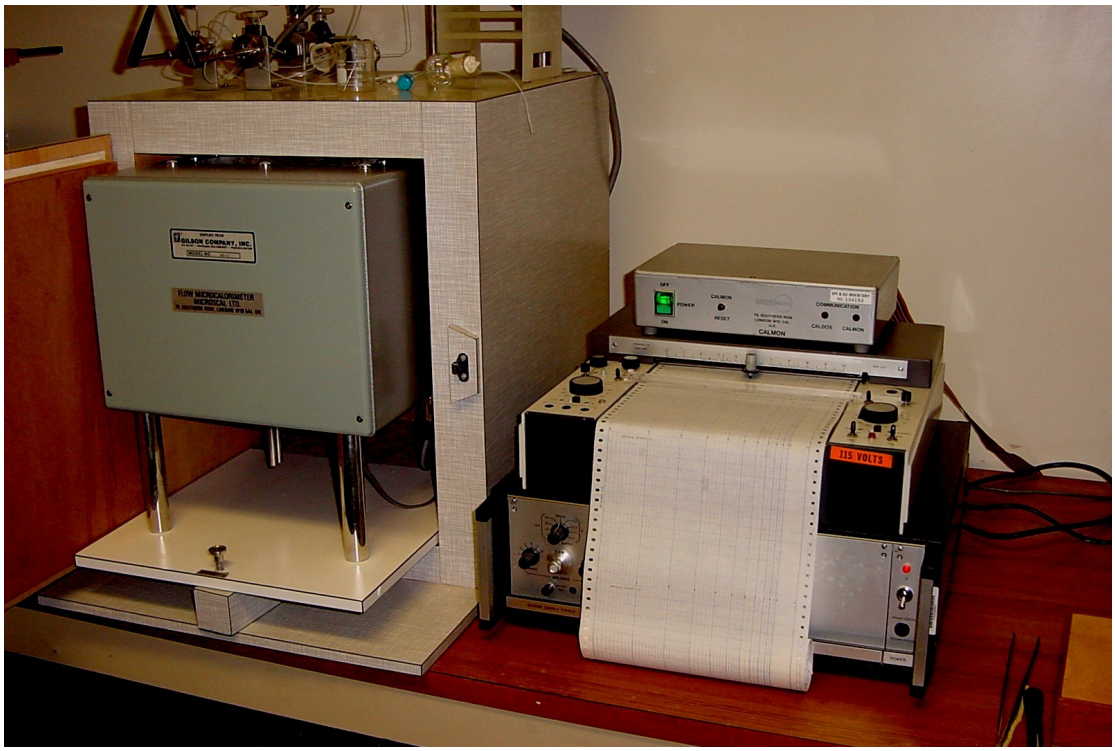

Figure 3.1. Microscal Flow Microcalorimeter.

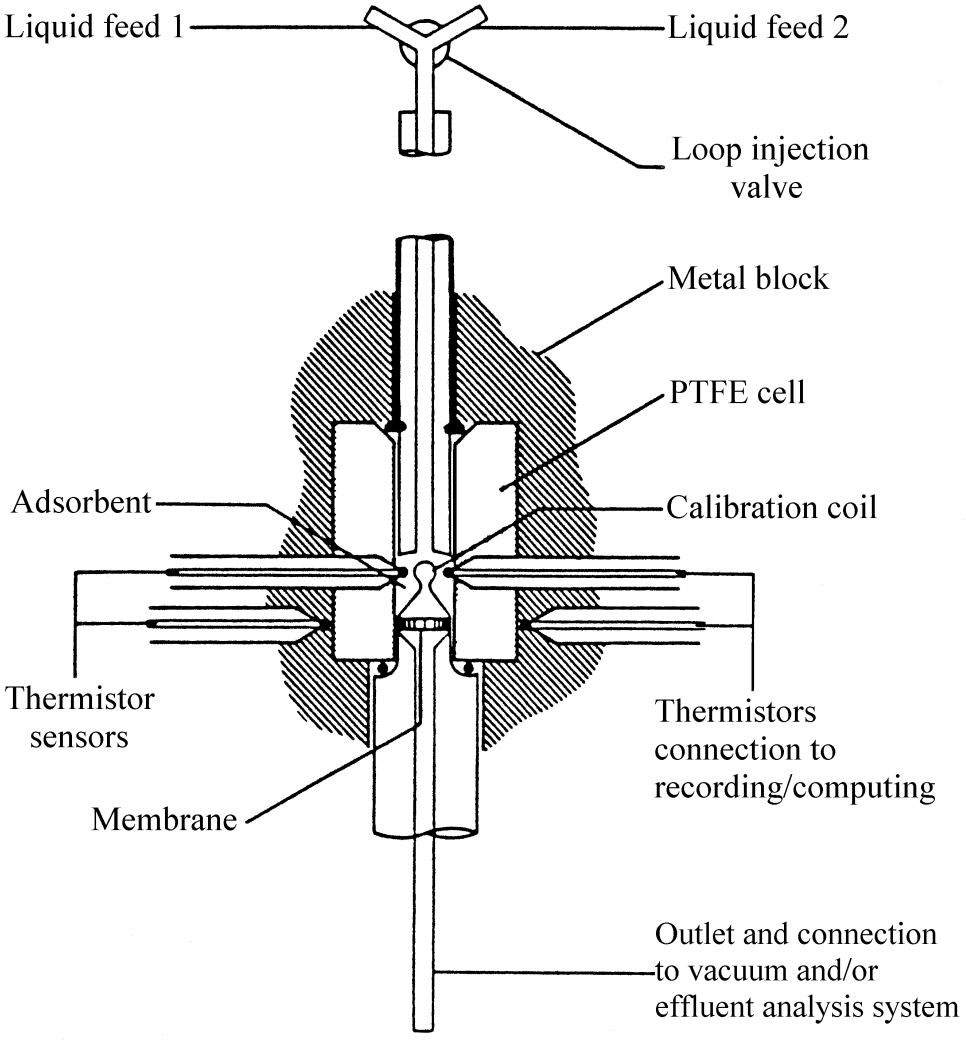

Figure 3.2. Schematic diagram of the flow microcalorimeter used for the heat of immersion measurements.

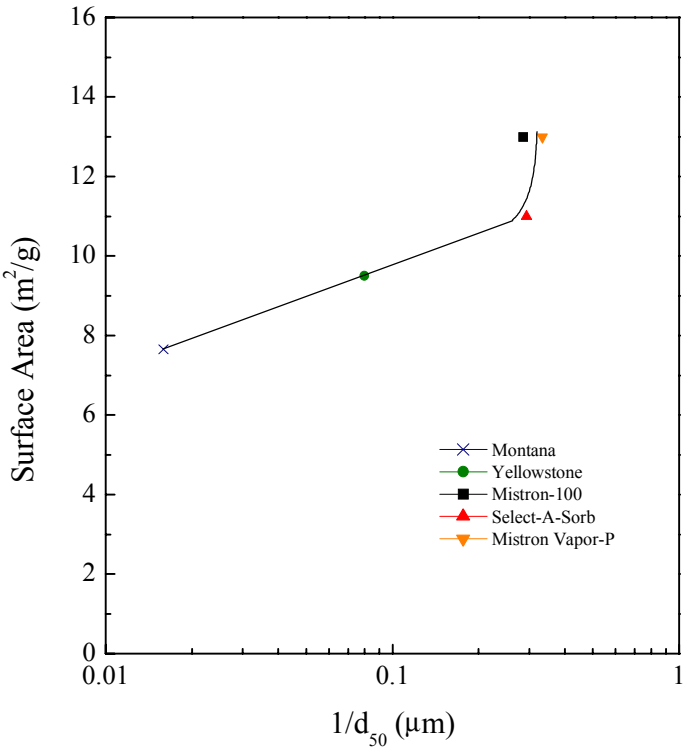

Figure 3.3. Surface area vs. $1/d_{50}$ for the talc samples.

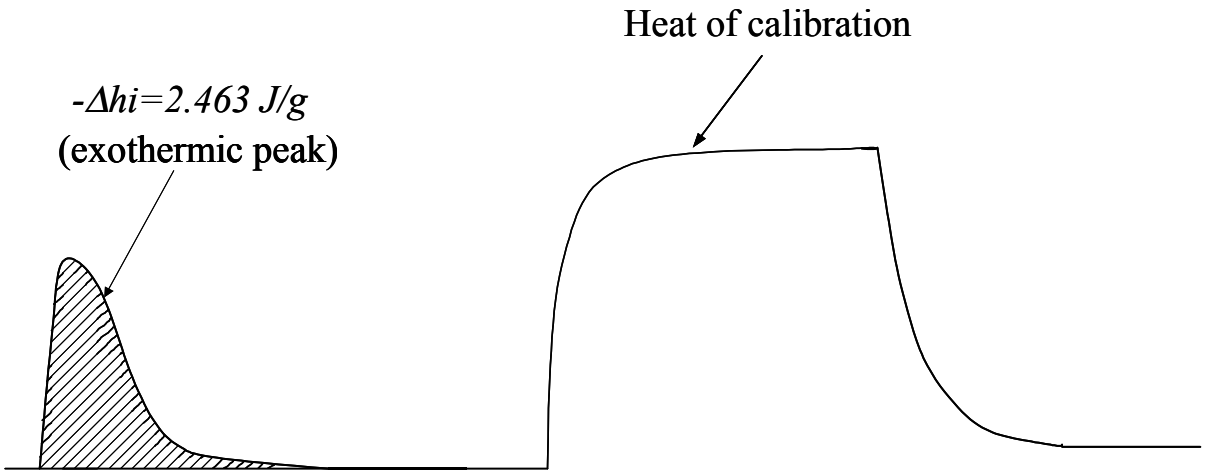

Figure 3.4. Typical thermal output of flow microcalorimeter including heat of immersion in water and heat of calibration peaks obtained for run-of-mine Montana talc sample. Areas under the curves are proportional to the heat created.

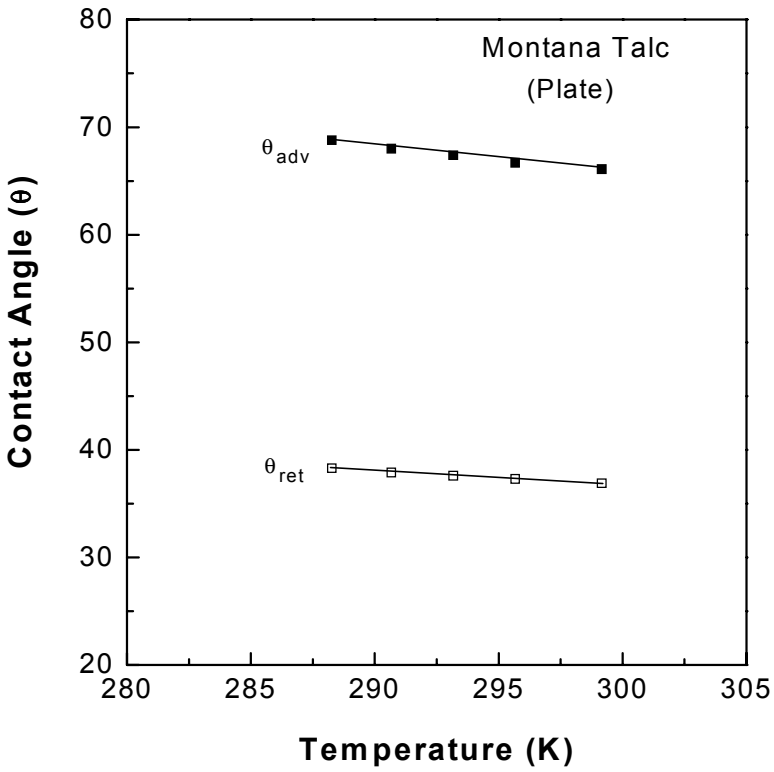

Figure 3.5. Advancing and retreating contact angles of water on Montana talc as a function of temperature, measured using Wilhelmy plate technique.

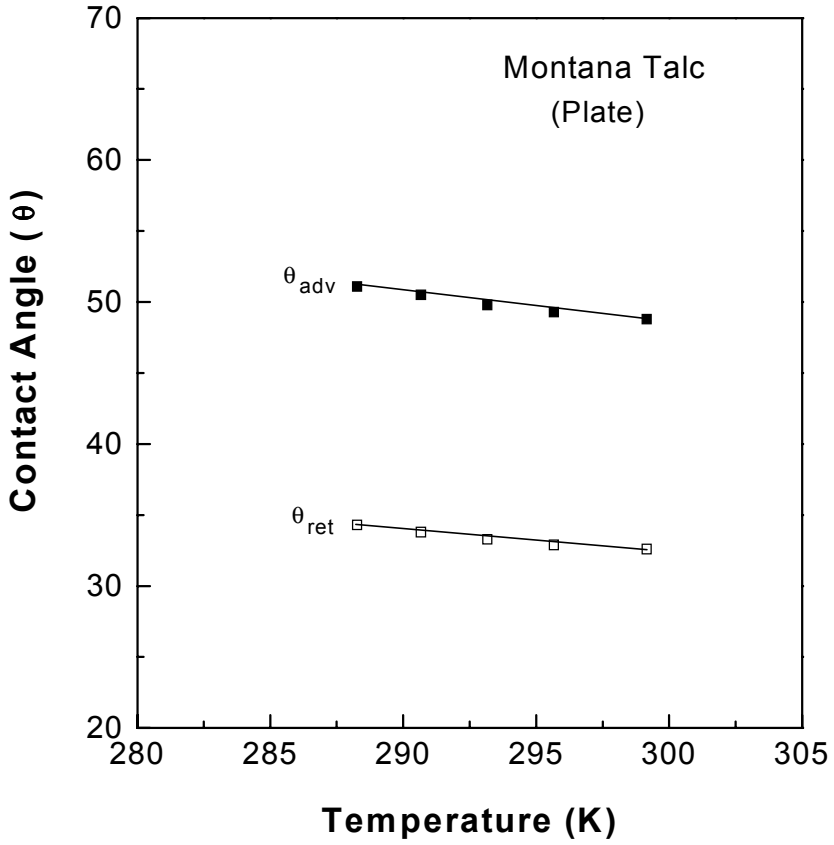

Figure 3.6. Advancing and retreating contact angles of formamide on Montana talc as a function of temperature, as measured using KSV Sigma70.

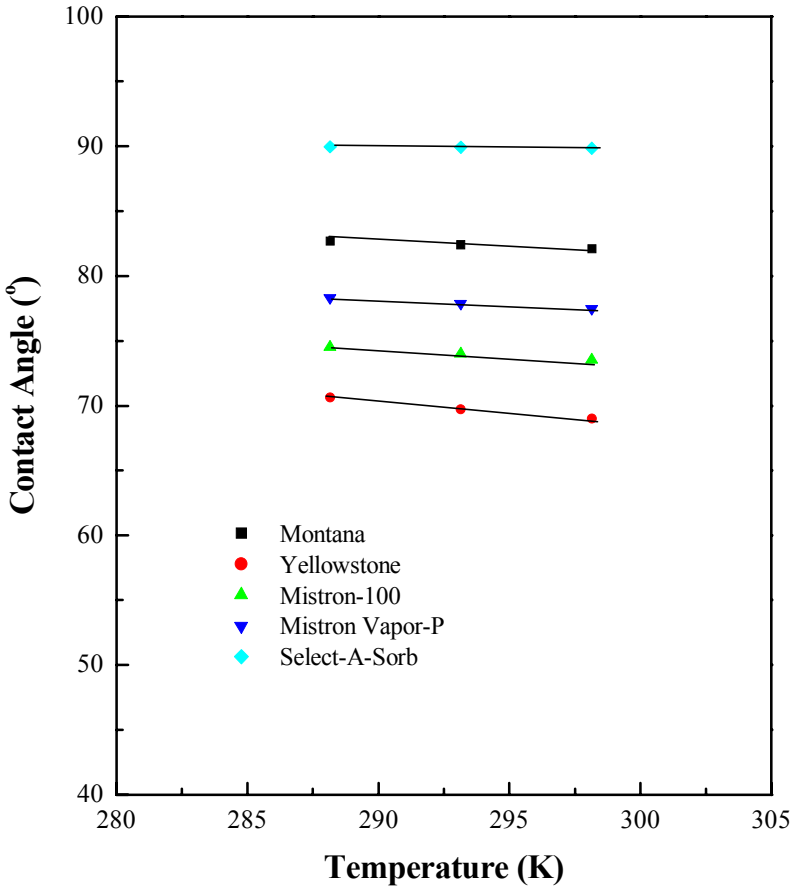

Figure 3.7. Advancing contact angles of water on various talc powders as a function of temperature, measured using capillary rise technique

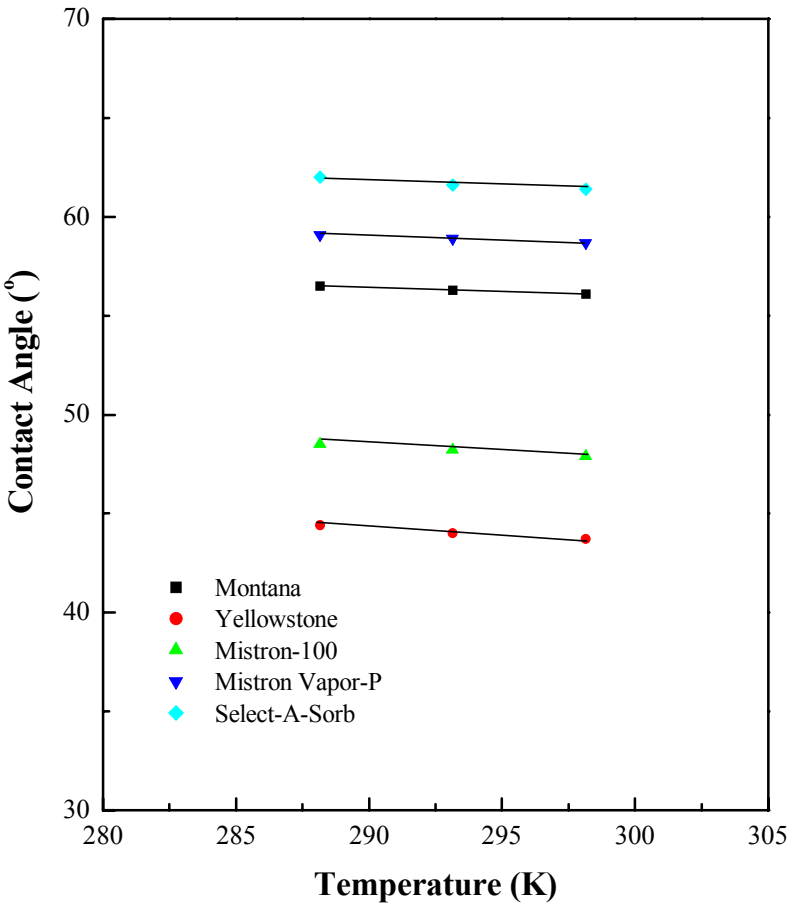

Figure 3.8. Advancing contact angles of formamide on various talc powders as a function of temperature, measured using capillary rise technique

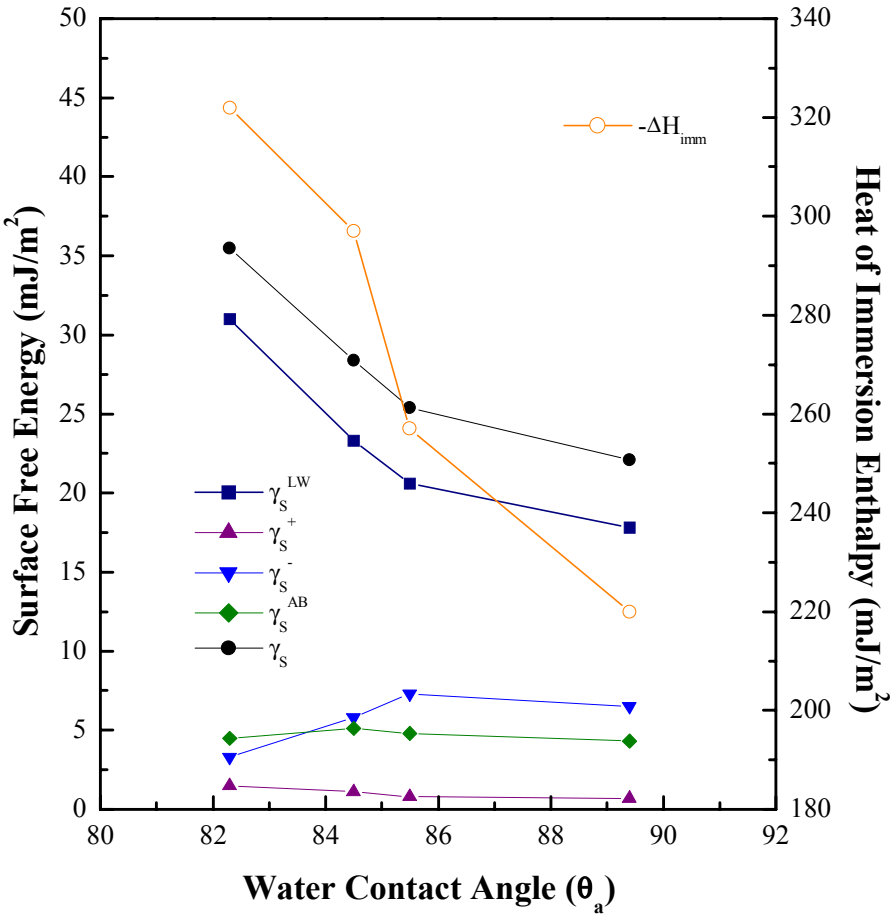

Figure 3.9. The heat of immersion enthalpies in water obtained from Table 3.2 and the surface free energy components obtained from Tables 2.10 and 2.12, plotted as a function of θ_a.